Pergamon

0301-9322(95)00075-5

Int. J. Multiphase Flow Vol. 22, No. 3, pp. 593–612, 1996

0301-9322/96 $15.00 + 0.00

THERMOCAPILLARY BUBBLE MIGRATION—THERMAL BOUNDARY LAYERS FOR LARGE MARANGONI NUMBERS

R. BALASUBRAMANIAM[1]†‡ and R. S. SUBRAMANIAN[2]

[1]Department of Mechanical and Aerospace Engineering, Case Western Reserve University, Cleveland, OH 44106, U.S.A.

[2]Department of Chemical Engineering, Box 5705, Clarkson University, Potsdam, NY 13699-5705, U.S.A.

(Received 12 April 1995; in revised form 8 November 1995)

Abstract—The migration of an isolated gas bubble in an immiscible liquid possessing a temperature gradient is analyzed in the absence of gravity. The driving force for the bubble motion is the shear stress at the interface which is a consequence of the temperature dependence of the surface tension. The analysis is performed under conditions for which the Marangoni number is large, i.e. energy is transferred predominantly by convection. Velocity fields in the limit of both small and large Reynolds numbers are used. The thermal problem is treated by standard boundary layer theory. The outer temperature field is obtained in the vicinity of the bubble. A similarity solution is obtained for the inner temperature field. For both small and large Reynolds numbers, the asymptotic values of the scaled migration velocity of the bubble in the limit of large Marangoni numbers are calculated. The results show that the migration velocity has the same scaling for both low and large Reynolds numbers, but with a different coefficient. Higher order thermal boundary layers are analyzed for the large Reynolds number flow field and the higher order corrections to the migration velocity are obtained. Results are also presented for the momentum boundary layer and the thermal wake behind the bubble, for large Reynolds number conditions. Copyright © 1996 Elsevier Science Ltd.

Key Words: thermocapillary migration, bubbles and drops, Marangoni convection, boundary layers, asymptotic analysis

1. INTRODUCTION

With the advent of the space program and the potential for space processing, there has been considerable interest in the motion of bubbles and drops in reduced gravity, both for fundamental understanding and actual applications (see review papers cited below). Thermally-induced surface tension gradient driven flow is the most often studied (and encountered) mechanism for this motion. When a bubble or drop is placed in a continuous phase in which a temperature gradient exists, the variation of interfacial tension with temperature along the interface will lead to a tangential stress. This stress will cause the motion of neighboring fluid and will lead to propulsion of the bubble in the direction of warmer fluid since surface tension decreases with temperature in most common fluids. Such motion is termed "thermocapillary migration" and forms the subject of the present study.

The two most important parameters governing thermocapillary motion are the Reynolds and Marangoni numbers. The Reynolds number is $\mathrm{Re} = V_R R_1/\nu$ and the Marangoni number is $\mathrm{Ma} = V_R R_1/\alpha$. Here R_1 is the radius of the bubble, ν and α are the kinematic viscosity and the thermal diffusivity of the surrounding liquid. The characteristic velocity $V_R = (-\sigma_T)AR_1/\rho\nu$ where σ denotes the surface tension, σ_T is the rate of change of surface tension with temperature (assumed to be a constant, typically negative, in this analysis) and A is the temperature gradient in the liquid. In thermocapillary migration, the Marangoni number serves the role of a Péclet number, its magnitude signifying the relative importance of convective transport of energy when compared to conduction.

Young *et al.* (1959) performed pioneering theoretical and experimental work on air bubbles in a silicone oil under conditions of negligible Reynolds and Marangoni numbers. Much has been

†Resident Research Associate at NASA Lewis Research Center, Cleveland, OH 44135, U.S.A.
‡To whom correspondence should be addressed.

done subsequently and most of the existing literature has been reviewed in Wozniak *et al.* (1988) and Subramanian (1992). Bratukhin (1976) and Thompson *et al.* (1980) attempted to improve upon the solution of Young *et al.* by a regular perturbation scheme in the Reynolds number, so as to include effects of inertia and shape deformations. Subramanian (1981) pointed out that the above regular perturbation approach is unable to satisfy the far-field condition on the temperature field at higher orders and obtained a solution of the energy equation for small values of the Marangoni number by the method of matched asymptotic expansions. Crespo & Manuel (1983) and Balasubramaniam & Chai (1987) showed that the solution of Young *et al.* is an exact solution of the momentum equation for any Reynolds number, so long as the Marangoni number is negligible. The latter authors also calculated the small deformations of a drop from a spherical shape. Numerical calculations of the velocity and temperature fields for a spherical bubble as well as the bubble velocity have been performed by Szymczyk & Siekmann (1988), Shankar & Subramanian (1988) and Balasubramaniam & Lavery (1989), and the deformation of a bubble and its impact on the migration velocity have been calculated by Haj-Hariri *et al.* (1990), Chen & Lee (1992) and Nas & Tryggvason (1993). The transient migration of a drop from an initial state of rest to the steady state has been analyzed by Dill & Balasubramaniam (1992).

The objective of the present study is to analyze the motion of an isolated gas bubble subjected to a uniform temperature gradient under zero gravity conditions when the Marangoni number is large. We consider two limiting cases, $\mathrm{Re}\to 0$ and $\mathrm{Re}\to\infty$. Physically, the former is the case of a highly viscous flow of a large Prandtl number fluid ($\mathrm{Pr} = \nu/\alpha$). The latter corresponds to an inertia-dominated flow of a fluid of low to moderate Prandtl number. An example of the first is the movement of a bubble of radius 5 mm in a silicone oil (which is a model fluid used in many terrestrial and space-flight experiments) of nominal kinematic viscosity 50 centistokes that is subjected to a temperature gradient of 1 K/mm. The Reynolds number in this case is around 0.5 and the Marangoni number is around 240. An example for the small Prandtl number case is the motion of a bubble of radius 2 mm in a melt of the semiconductor silicon with a temperature gradient of 2.5 K/mm. Here the Reynolds number is around 1700 and the Marangoni number is roughly 50.

It is assumed that the bubble–liquid interface is clean and free from surfactants. Several such interfaces have been experimented with in the context of surface-driven motion and bubble migration, notably the air–silicone oil interface. Bubbles are also modeled as undeformed spheres in this analysis. In the large Pr example given above, the Capillary number ($\mathrm{Ca} = \rho\nu V_R/\sigma$) is 0.01 and deformation is negligible. In the small Pr example the Capillary number is 0.003, but the Weber number (ReCa) is not small and deformations may not be neglected. However experimental and numerical evidence thus far suggests that deformation is negligible and nowhere near what is observed for gravity-driven motion. Nas & Tryggvason (1993) performed a two-dimensional calculation with $\mathrm{Re} = 2000$, $\mathrm{Ma} = 400$ and $\mathrm{Ca} = 0.0166$ and report negligible deformations. Also no flow separation is evident even at $\mathrm{Re} = 2000$ in the calculations by Nas & Tryggvason and Balasubramaniam & Lavery.

To keep the analysis tractable it is assumed that viscosity is not a function of temperature. While viscosity changes due to temperature variations can be important in virtually all experiments, a largely successful approach in prediction of the bubble velocity has been to consider such variation "quasi-static", i.e. a local value of the viscosity is used in an expression obtained from a theory which assumes constant viscosity.

In cases of both small and large Re, for large Ma, convective energy transport dominates over conduction almost everywhere. It will be seen that a thermal boundary layer must exist near the bubble surface in order to satisfy the boundary conditions. In the analogous fluid mechanical problem in the limit $\mathrm{Re}\to\infty$ (Chao 1962; Moore 1963), the boundary layer results in $O(1)$ change in the stress; the velocity changes in the boundary layer are small, of $O(\mathrm{Re}^{-1/2})$. In constrast, it will be shown that the thermal boundary layer produces temperature field changes of $O(1)$ here.

A key question is the dependence of the scaled bubble velocity on Ma. From their numerical results for the temperature field under negligible Re, Shankar & Subramanian (1988) conclude that the scaled bubble velocity v_∞ (non-dimensionalized by the velocity scale V_R) shows a logarithmically decreasing behavior with Ma in the range $20 \leqslant \mathrm{Ma} \leqslant 200$. A fit to the numerical results of the form $v_\infty = 1.59/(1.84 + \ln \mathrm{Ma})$ was found to be indistinguishable from the numerical results in

that range. The extrapolated value of v_∞ from this fit goes to zero as Ma becomes infinite. Balasubramaniam & Lavery (1989) performed numerical computations in the range $0 \leqslant \mathrm{Ma} \leqslant 1000$, $0 \leqslant \mathrm{Re} \leqslant 2000$. Their results show that while v_∞ decreased with increasing Ma at fixed Re in this range, no clear asymptotic behavior could be discerned.

While the present analysis was under way, Crespo & Jiménez-Fernández (1991, 1992) have performed thermal boundary layer analyses for large Ma using velocity fields applicable in the limits of both small and large Re. Their analysis is very similar to ours presented in section 3. It will be shown that their result for the large Re case is in agreement with the present solution. However, their result for the Re→0 case appears to be in error in the numerical calculations for the Fourier coefficients in the series expansion of the velocity field. Also, in the case of large Re, we present the higher order corrections to the bubble migration velocity.

In what follows, section 2 summarizes the known velocity fields for small and large Re, section 3 deals with the boundary layer formalism for the leading order temperature field and section 4 deals with the higher order thermal boundary layers for the large Re flow field. The results are discussed in section 5 and some concluding remarks are made in section 6. The momentum boundary layer for large Re is discussed in appendix A and the thermal wake for large Reynolds numbers is analyzed in appendix B.

2. VELOCITY FIELDS FOR SMALL AND LARGE REYNOLDS NUMBERS

Subramanian (1981) has analyzed the thermocapillary migration of a gas bubble in the limit of zero Reynolds number and small Marangoni numbers. The general solution for the flow field appropriate to axisymmetric thermocapillary migration problems in a reference frame traveling with the bubble is reproduced below from that analysis (see also Levan & Newman 1976). Thus the scaled flow variables in the limit of small Re are given by

$$\psi(r,\mu) = \frac{1}{4}(1-\mu^2)I_2\left(\frac{1}{r}-r^2\right) + \frac{1}{4}\sum_{n=3}^{\infty} n(n-1)I_n\left(\frac{1}{r^{n-1}}-\frac{1}{r^{n-3}}\right)C_n(\mu) \qquad [1]$$

$$u(r,\mu) = \frac{I_2}{2}\mu\left(1-\frac{1}{r^3}\right) + \frac{1}{4}\sum_{n=3}^{\infty} n(n-1)I_n\left(\frac{1}{r^{n-1}}-\frac{1}{r^{n+1}}\right)P_{n-1}(\mu) \qquad [2]$$

$$v(r,\mu) = -\frac{I_2}{4}(1-\mu^2)^{1/2}\left(2+\frac{1}{r^3}\right) + \frac{1}{4}\sum_{n=3}^{\infty} n(n-1)I_n\left(\frac{n-3}{r^{n-1}}+\frac{1-n}{r^{n+1}}\right)\frac{C_n(\mu)}{(1-\mu^2)^{1/2}} \qquad [3]$$

Lengths are scaled by the bubble radius R_1 and velocities by V_R defined earlier. The scaled radial coordinate is r and $\mu = \cos\theta$. The polar angle θ is measured from the front stagnation streamline. The scaled radial and tangential velocities are u and v, respectively, and ψ is the scaled streamfunction. $C_n(\mu)$ and $P_n(\mu)$ are the Gegenbauer function of order n and degree $-1/2$ and the Legendre polynomial of order n, respectively. The Fourier coefficients I_n are obtained from the temperature field on the bubble surface:

$$I_n = -\int_{-1}^{1} C_n(\mu)\frac{\partial T}{\partial \mu}(1,\mu)\,\mathrm{d}\mu \quad n \geqslant 2 \qquad [4]$$

Here, T is a transformed temperature related to the physical temperature $\hat{T}$ by $T = (\hat{T} - Av_\infty V_R t)/(AR_1)$, where A is the temperature gradient far away from the bubble and t is time. The scaled bubble migration velocity is

$$v_\infty = -\frac{I_2}{2} = \frac{1}{4}\int_{-1}^{1}(1-\mu^2)\frac{\partial T}{\partial \mu}(1,\mu)\,\mathrm{d}\mu \qquad [5]$$

which is obtained from the condition that the net hydrodynamic force on the migrating bubble is zero.

When the Reynolds number is large, the velocity field may be approximated by a potential flow field. As in body force driven motion (Levich 1962), there is a thin boundary layer near the bubble surface in the stress field in order to satisfy the tangential stress balance at the surface (unlike in body force-driven motion, the surface shear stress in non-zero and equals the surface tension

gradient). However, the velocity field, to leading order, is that corresponding to potential flow all the way to the bubble surface. The correction to this field in the boundary layer occurs at $O(\mathrm{Re}^{-1/2})$ as discussed in appendix A, and is neglected in the present analysis.

The potential flow field does not exert any force on the bubble regardless of the bubble velocity. Thus an alternate condition is required to calculate v_∞. This is provided by viscous dissipation arguments (Levich 1962; Crespo & Manuel 1983; Balasubramaniam 1987)—at steady state migration, the rate at which work is done by the surface tension force equals the rate at which energy is dissipated by viscosity.

Thus the large Reynolds number flow field, again in a reference frame traveling with the bubble, is given below

$$\psi(r,\theta)=\frac{v_\infty}{2}\sin^2\theta\left(r^2-\frac{1}{r}\right)\quad u(r,\theta)=-v_\infty\cos\theta\left(1-\frac{1}{r^3}\right)$$

$$v(r,\mu)=v_\infty\sin\theta\left(1+\frac{1}{2r^3}\right) \qquad [6]$$

The scaled bubble velocity is

$$v_\infty=\frac{1}{4}\int_{-1}^{1}(1-\mu^2)\frac{\partial T}{\partial\mu}(1,\mu)\,\mathrm{d}\mu \qquad [7]$$

where the latter is obtained by the dissipation argument mentioned above. It may be noticed that [6] and [7] for the large Re case may be obtained from [1], [4] and [5] for the small Re case formally by setting $I_n=0, n\geqslant 3$. Thus the large Re problem may be treated as a special case of the small Re problem in this analysis.

3. LEADING ORDER TEMPERATURE FIELD

The temperature gradient far away from the bubble is assumed to be a constant. Typically, the temperature coefficient of surface tension, $\mathrm{d}\sigma/\mathrm{d}T$, is negative. The bubble would then move toward the warm portion of the surrounding liquid. In a reference frame moving with the bubble, the temperature field is unsteady because the field at infinity is unsteady in this reference frame. However, a modified temperature field obtained by subtracting from it the undisturbed temperature field evaluated at the center of the bubble will approach a steady field at infinity and therefore will achieve a steady state (Subramanian 1981). Thus the energy equation for this steady field $T(r,\theta)$ may be written as (Balasubramaniam & Chai 1987)

$$v_\infty+u\frac{\partial T}{\partial r}+\frac{v}{r}\frac{\partial T}{\partial\theta}=\frac{1}{\mathrm{Ma}}\nabla^2T \qquad [8]$$

with boundary conditions

$$\frac{\partial T}{\partial r}(1,\mu)=0 \qquad [9]$$

i.e. the bubble surface is adiabatic,

$$T\to r\mu \quad \text{as } r\to\infty \qquad [10]$$

i.e. the temperature field approaches the undisturbed field far away. In [8], u and v are given by [2] and [3] and v_∞ is obtained from [5].

Equations [8]–[10], for known v_∞, are linear. Nevertheless analytical solution is formidable and we resort to perturbation theory for solution in the limit $\mathrm{Ma}\to\infty$. For well-known reasons, the perturbation is singular, and therefore we use the method of matched asymptotic expansions. For large Ma, one would expect a radial thermal boundary layer to be present near the bubble surface. As usual, the temperature field outside the boundary layer is called the outer temperature field and that within the boundary layer is termed the inner temperature field.

3.1. Outer temperature field

Let

$$\epsilon^2 = \frac{1}{\mathrm{Ma}} \tag{11}$$

$$I_n = I_{n0} + o(1) \quad n \geqslant 2 \tag{12}$$

$$u = u_0 + \cdots \tag{13}$$

$$v = v_0 + \cdots \tag{14}$$

$$\psi = \psi_0 + \cdots \tag{15}$$

$$T(r, \mu) = T_0(r, \mu) + \cdots \tag{16}$$

where T is the outer temperature field. Substituting [13]–[16] in [8], the energy equation to leading order is

$$v_{\infty 0} + u_0 \frac{\partial T_0}{\partial r} - \frac{v_0}{r}(1-\mu^2)^{1/2} \frac{\partial T_0}{\partial \mu} = 0 \tag{17}$$

$$T_0 \to r\mu \quad \text{as } r \to \infty \tag{18}$$

Transforming from (r, μ) to (r, ψ_0) coordinates where ψ is the streamfunction, the solution may be written as

$$T_0(r, \mu) = r\mu + \int_{\infty}^{r} \frac{1}{u_0}(-v_{\infty 0} + v_0 \sin\theta - u_0 \cos\theta)\, \mathrm{d}_{\tilde{r}} \tag{19}$$

where the integrand must be expressed as a function of $(\tilde{r}, \psi_0)$. This may be further specialized for the large Re flow field to be

$$T_0(r, \mu) = r\mu + \int_{r}^{\infty} \frac{1}{(\tilde{r}^3 - 1)} \frac{\left(\dfrac{3\psi_0}{v_{\infty 0}(\tilde{r}^2 - 1/\tilde{r})} - 1\right)}{\left(1 - \dfrac{2\psi_0}{v_{\infty 0}(\tilde{r}^2 - 1/\tilde{r})}\right)^{1/2}} \mathrm{d}\tilde{r} \tag{20}$$

We are unable to find a closed form result for the integrals in [19] or [20]. Specialized results may be obtained for (i) $r \gg 1$ and (ii) $\theta = 0, \pi$ for large Re. As can be expected, the outer solution is unable to satisfy the boundary conditions at the bubble surface and a thermal boundary layer exists there. To analyze this boundary layer and perform the necessary matching, the outer solution is needed near the bubble surface. We obtain it below via an expansion of the velocities near $r = 1$.

3.1.1. Outer field near $r = 1$. Near $r = 1$, the leading order results for the velocities may be expanded as

$$u_0(r, \mu) = \frac{3}{2} I_{2_0} \mu (r-1) + \frac{r-1}{2} \sum_{n=3}^{\infty} n(n-1) I_{n_0} P_{n-1}(\mu) + O((r-1)^2) \tag{21}$$

$$v_0(r, \mu) = -\frac{3}{4}(1-\mu^2)^{1/2} I_{2_0} - \frac{1}{2} \sum_{n=3}^{\infty} n(n-1) I_{n_0} \frac{C_n(\mu)}{(1-\mu^2)^{1/2}} + O(r-1) \tag{22}$$

Using these in [17], the solution for T_0 can be obtained as

$$T_0(r, \mu) = \frac{1}{A_0} \ln(r-1) + \ln(f(\mu)) + g(\psi) \tag{23}$$

$$A_0 = 3 - \frac{1}{2v_{\infty 0}} \sum_{n=3}^{\infty} n(n-1) I_{n_0} \tag{24}$$

$$\frac{1}{f}\frac{df}{d\mu} = \frac{-v_{\infty 0} + \frac{3}{A_0}v_{\infty 0}\mu - \frac{1}{2A_0}\sum_{n=3}^{\infty} n(n-1)I_{n_0}P_{n-1}(\mu)}{-\frac{3}{2}v_{\infty 0}(1-\mu^2) + \frac{1}{2}\sum_{n=3}^{\infty} n(n-1)I_{n_0}C_n(\mu)} \qquad [25]$$

The condition $\partial T_0/\partial\theta = 0$ at $\theta = 0$ has been used in the above solution. Since $\psi = 0$ on the bubble surface, $g(\psi)$ is merely a constant. For the large Re case, it can be established that

$$A_0 = 3, \quad f(\mu) = (1+\mu)^{2/3}, \quad g = 1 + \frac{\pi}{6\sqrt{3}} - \frac{1}{6}\ln 48 \qquad [26]$$

The value of g is obtained by connecting the solution for T_0 from [23] to that given by [20] along the front stagnation streamline. The solution for T_0 given above satisfies neither [9] nor [10]. The result is good only as $r \to 1$ and cannot be expected to satisfy the condition as $r \to \infty$. The adiabatic condition at the bubble surface cannot be satisfied as the order of the governing equation has been reduced. In fact, the outer field exhibits a logarithmic singularity as the bubble surface is approached. In order to satisfy the boundary condition at the bubble surface, we shall develop an inner expansion near $r = 1$. $\partial T_0/\partial\theta$ does not have a singularity near $\theta = 0$ (in fact it is zero). Thus there is no tangential boundary layer near the forward stagnation point.

It is seen that $f(\mu)$ has a singularity at $\mu = -1$; hence a boundary layer (really a thermal wake) must exist in the angular coordinate near $\theta = \pi$. The thermal wake is analyzed in appendix B for the large Re flow field. It is shown there that the boundary layer thickness is proportional to ϵ. However, the singularity is sufficiently weak that integrals needed for evaluating the bubble migration velocity can be obtained without analyzing the thermal wake; from [4] it can be shown that the thermal wake contributes to the bubble migration velocity only at $O(\epsilon^2)$.

3.2. The inner temperature field

In order to satisfy the adiabatic boundary condition at the bubble surface, we need to include the neglected conduction term in the radial direction. This is accomplished by suitably stretching the radial distance from the bubble surface in an inner (boundary layer) solution. One might wonder whether θ-conduction is also necessary near the forward stagnation point to relieve the singularity in the outer solution. The answer is negative. It will be seen from the solution in this section that radial conduction alone is sufficient. The physical interpretation is that fluid particles on the bubble surface do not infer their temperatures via θ-conduction from the forward stagnation point. Rather, they infer their temperatures via radial conduction across the boundary layer from streamlines adjoining the stagnation streamline. The fluid velocity is non-zero everywhere on these streamlines and from the outer solution, the temperature along them is bounded.

We define inner variables (x, μ) via $x = (r-1)/\epsilon$ and write the inner temperature field $t(x, \mu)$ as

$$t(x, \mu) = t_0(x, \mu) + o(1) \qquad [27]$$

The energy equation at leading order is

$$v_{\infty 0} + \left(\frac{\partial u_0}{\partial r}(1, \mu)\right)x\frac{\partial t_0}{\partial x} - (1-\mu^2)^{1/2}v_0(1, \mu)\frac{\partial t_0}{\partial \mu} = \frac{\partial^2 t_0}{\partial x^2} \qquad [28]$$

$$\text{At} \quad x = 0 \quad \frac{\partial t_0}{\partial x} = 0; \qquad \text{at } \theta = 0 \quad \frac{\partial t_0}{\partial \theta} = 0 \qquad [29]$$

and as $x \to \infty$, t_0, the inner temperature field, must match the outer field. A transformation is made from (x, μ) coordinates to (η, ξ) coordinates where

$$\eta = (1-\mu^2)^{1/2}v_0(1, \mu)x \qquad [30]$$

$$\xi = \frac{3}{4}I_{2_0}\left(\mu - \frac{\mu^3}{3} - \frac{2}{3}\right) + \frac{1}{2}\sum_{n=3}^{\infty}\frac{n(n-1)}{(2n-1)}I_{n_0}(C_{n+1}(\mu) - C_{n-1}(\mu)) \qquad [31]$$

($\xi(\mu)$ is such that $\xi'(\mu) = -v_0(1, \mu)(1-\mu^2)^{1/2}$, $\xi(1) = 0$). η is related to the streamfunction. This transformation reduces the energy equation given above to a diffusion equation with a sink term. It is straightforward to find a solution for t_0 as

$$t_0 = C_1 + \ln(f(\mu)) - \frac{1}{A_0}\ln(-\xi') + \frac{1}{2K}\ln\xi + \frac{2}{K}F(\zeta) \qquad [32]$$

where

$$\zeta = \frac{\eta}{2\sqrt{\xi}}, \quad F(\zeta) = \int_0^\zeta \mathrm{D}(w)\,\mathrm{d}w = \int_0^\zeta \mathrm{e}^{-w^2}\left(\int_0^w \mathrm{e}^{z^2}\,\mathrm{d}z\right)\mathrm{d}w \qquad [33]$$

C_1 and K are arbitrary constants that will be determined by matching with the outer solution. $\mathrm{D}(w)$ is Dawson's function (Abramowitz & Stegun 1968).

3.2.1. Matching. The result for the outer field T_0 from [23] written in inner variables, truncated at $O(1)$ in ϵ and rewritten in outer variables is unchanged. The inner result for t_0 from [32] written in outer variables and truncated at $O(1)$ is given below (we use the result that for large ζ, $\mathrm{D}(\zeta)\to 1/2\zeta$, and hence $F(\zeta)\to\frac{1}{2}\ln\zeta$)

$$t_0 = C_1 + \ln(f(\mu)) + \left(\frac{1}{K} - \frac{1}{A_0}\right)\ln(-\xi') + \frac{1}{K}\ln\left(\frac{r-1}{2\epsilon}\right) \qquad [34]$$

Thus matching requires that

$$K = A_0 \qquad [35]$$

$$C_1 = \frac{1}{A_0}\ln\epsilon + C_2 \qquad [36]$$

Even though the inner expansion was initially assumed to be of the form given in [27], the lack of a $\ln\epsilon$ term in the outer result forces the choice of C_1 in [36] to include $(1/A_0)\ln\epsilon$. C_2 is an $O(1)$ constant, the value of which cannot be established unless the outer solution near $r = 1$ is known in more detail, including all the constants. It is straightforward to establish that at $O(\ln\epsilon)$, the only contribution to the inner field is $(1/A_0)\ln\epsilon$.

The appearance of $\ln\epsilon$ at leading order in the inner solution requires discussion. A uniformly valid expansion can be constructed by additive composition from the inner and outer temperature fields. Since the outer field we have given ([23]) is good only near $r = 1$, the composite expansion in this region is merely the inner field. The temperature on the surface of the bubble becomes singular (negative infinity) in the limit of $\epsilon\to 0$. Of course, in physical systems there is always some non-zero conductivity. Therefore the surface temperatures will remain finite.

The reason for the relatively cold conditions prevalent at the surface of the bubble for small ϵ can be understood by examining the behavior of a thin bundle of fluid elements surrounding the front stagnation streamline. As the fluid elements approach the bubble from far away, we infer from [17] that in the outer region they lose heat and get colder owing to the presence of the sink (the $v_{\infty 0}$ term). The reduction in temperature is proportional to the transit time of the fluid elements since the sink is constant. This is especially pronounced near the front stagnation point where the velocity approaches zero and the transit time diverges logarithmically. When the elements in the bundle reach the inner region, they communicate the temperature information by conduction to the elements on the bubble surface. Consequently the fluid elements on the bubble surface become cold as well.

The correctness of the above results is qualitatively supported by isotherms sketched from the numerical solutions of the problem (Shankar & Subramanian 1988; Balasubramaniam & Lavery 1989). It is seen that the scaled temperatures on the bubble surface decrease as the Marangoni number is increased. The increase is gradual as one might anticipate because of the $\ln\epsilon$ dependence. However a precise $\ln\epsilon$ behavior cannot be established from the numerical results as the computations have not been performed beyond Ma = 1000.

3.3. I_n calculations

The unknown Fourier coefficients at leading order $I_{n_0}, n \geqslant 2$ are calculated using [4]. It can be shown that

$$\frac{\partial T}{\partial \mu}(1, \mu) = \frac{\partial t_0}{\partial \mu}(0, \xi) = -\frac{v_{\infty 0}}{\xi'} + \frac{\xi'}{2A_0 \xi} \qquad [37]$$

where $\xi(\mu)$ is given by [31]. Thus the Fourier coefficients are given by

$$I_{n_0} = -\int_{-1}^{1} C_n(\mu)\left(-\frac{v_{\infty 0}}{\xi'} + \frac{\xi'}{2A_0 \xi}\right) \mathrm{d}\mu \quad n \geqslant 2 \qquad [38]$$

This constitutes a non-linear system of algebraic equations for the unknown Fourier coefficients and must be solved numerically, after truncation of the infinite series at a large but finite value of n (say $n = N$).

A very similar analysis was used by Crespo & Jiménez-Fernández (1991, 1992) to calculate the migration velocity in the limits of Re$\to\infty$ and Re$\to$0, for large Marangoni numbers. Our solution for large Re is presented below and agrees with their solution. The results for Re$\to$0 are provided in section 3.3.2.

3.3.1. Results for the large Reynolds number flow field. For Re$\to\infty$, the inner temperature field may be written as

$$t_0(x, \theta) = \frac{1}{3}\ln \epsilon + 1 + \frac{\pi}{6\sqrt{3}} - \frac{1}{6}\ln(27 v_{\infty 0}^2) + \frac{2}{3}\ln\left(\frac{1+\cos\theta}{\sin\theta}\right) + \frac{1}{6}\ln\hat{\xi} + \frac{2}{3}F(\hat{\zeta}) \qquad [39]$$

$$\hat{\xi} = \frac{v_{\infty 0}}{2}(1-\mu)^2(2+\mu) \qquad [40]$$

$$\hat{\zeta} = \frac{3 v_{\infty 0}}{4\sqrt{\hat{\xi}}} x \sin^2\theta \qquad [41]$$

$$F(\hat{\zeta}) = \int_0^{\hat{\zeta}} \mathrm{D}(y)\, \mathrm{d}y \qquad [42]$$

$v_{\infty 0}$ is calculated from [5] and [37] as

$$v_{\infty 0} = \frac{1}{4}\int_0^{\pi}\left(-\frac{v_{\infty 0}}{\hat{\xi}'} + \frac{\hat{\xi}'}{6\hat{\xi}}\right)\sin^3\theta\, \mathrm{d}\theta \qquad [43]$$

which computes to

$$v_{\infty 0} = \frac{1}{3} - \frac{1}{8}\ln 3 = 0.196007 \qquad [44]$$

Note that [43] is the condition from energy dissipation arguments ([7]). Crespo & Jiménez-Fernández obtain the same equation when they require the mass flux in the θ direction in the momentum boundary layer to be bounded at $\theta = \pi$.

The above result for v_∞ is valid for Re$\gg$1 and Ma$\gg$1. Even though potential flow velocities have been used within the thermal boundary layer ([28]) for large Re, there is no restriction that the Prandtl number be small. This is because the momentum boundary layer is a layer where the shear stress (and not the velocity itself) undergoes a sharp change. As shown in appendix A, the correction to the potential flow velocity in the momentum boundary layer is $O(\mathrm{Re}^{-1/2})$. The leading order flow field everywhere (including the thermal boundary layer) is the potential flow field regardless of the Prandtl number.

3.3.2. Results for the small Reynolds number flow field. Since the velocity field in the limit Re$\to$0 is expressed in the form of an infinite series, the Fourier coefficients I_{n_0} cannot be calculated analytically and are determined numerically. The infinite series is truncated at a large value of $n = N$. Consistent results for $v_{\infty 0}$ have been obtained in the range $10 \leqslant N \leqslant 75$. The computations were carried out using successive approximations (i.e. fixed point iteration). Basically, a set of I_{n_0} is guessed and used in the right hand side of [38]. This then generates a new set of I_{n_0} and the process is repeated till convergence is achieved to a specified tolerance. Convergence is checked for I_{2_0} and

the ratio of the sum of the absolute values of the deviations in I_{n_0} in consecutive iterations to the sum of the current absolute values of I_{n_0}. Underrelaxation was used in obtaining the new set of I_{n_0}. The required integrals were calculated by Romberg integration (Burden *et al.* 1981). Typically seventeen Romberg steps were necessary for accuracy to four significant digits for the I_{n_0}.

It turns out that the computations are quite cumbersome. In fact, we discovered that direct use of [24] for the constant A_0 (A_0 is recalculated once a new set of I_{n_0} is obtained) is the cause of severe difficulties in the calculations. First, odd values of N do not yield a converged set of I_{n_0} by a fixed point iteration method; second, for even values of N between 10 and 150, the numerically determined values of both A_0 and $v_{\infty 0}$ diverge with N (they increase monotonically).

An issue to investigate in connection with the convergence difficulties mentioned above is that the temperature gradient on the bubble surface given by [37] is singular at the rear pole ($\theta = \pi$). The left-hand side of the energy equation ([8]) has a sink term which, along with the convective transport terms, must be balanced by conduction near stagnation points where the velocities go to zero. Conduction in the thin radial boundary layer accommodates the sink term at the forward stagnation point ($\theta = 0$). At $\theta = \pi$, the radial boundary layer is infinitely thick; consequently, there must exist a boundary layer in the angular coordinate near $\theta = \pi$ in order to balance the sink term. Since the conduction term in the angular direction drops out at leading order in [28] for the inner temperature field, the surface temperature gradient given by [37] must be singular at $\theta = \pi$. However, in the integrals for I_{n_0}, this gradient is weighted by $C_n(\mu)$; it can be shown that $C_n(\mu)\partial T/\partial \mu$ on the bubble surface is bounded everywhere. Thus, in spite of the singularity in $\partial T/\partial \mu$ at $\theta = \pi$, it should be possible to determine a set of I_{n_0}. This is precisely what happens for the large Re flow field.

As alluded to earlier, the source of the numerical difficulties is in the expression for A_0 ([24]). The series $\Sigma_{n=3}^{\infty} n(n-1)I_{n_0}$, and more generally the series $\Sigma_{n=3}^{\infty} n(n-1)I_{n_0}P_{n-1}(\mu)$, appear to have convergence problems. The constant A_0 and another constant related to it, viz. $B_0 = -3v_{\infty 0} - \frac{1}{2}\Sigma_{n=3}^{\infty}(-1)^{n-1}n(n-1)I_n$ are proportional to the viscous normal stress (represented by the series given above) at $\theta = 0, \pi$ respectively. We find that the series for B_0 is divergent. Thus the singularity of the normal stress on the bubble surface at $\theta = \pi$ is controlling the convergence of the series in the A_0 expression.

It is found that if A_0 is taken to be fixed during a fixed point iteration for I_{n_0} (i.e. A_0 is not recalculated after a new set of I_{n_0} is obtained), then the convergence problem for odd N mentioned above disappears. Furthermore, typical values of I_{n_0} thus obtained (non-converged, i.e. not summing up to the guessed value of A_0) are alternating in sign. Thus the series in [24] for A_0 is one of alternating sign and Euler's transformation (Meksyn 1961) can be used to improve the convergence of the series. The Euler summation procedure is used with Van Wijngaarden's algorithm (Press *et al.* 1986) for calculating A_0 (A_0 recalculated for every new set of I_{n_0}) together with underrelaxation in the fixed point iteration procedure (previous iterates weighted 60–90%). This yields a convergent set of I_{n_0} (with respect to N) for N in the range 10–75, both for odd and even N. The calculated values of I_{n_0} are presented in table 1. The final results are

$$v_{\infty 0} = 0.1538 \qquad [45]$$

$$A_0 = 2.406 \qquad [46]$$

It is worth making a comment regarding the integrand in the r.h.s. of [38] at the end point $\theta = \pi$. At first sight, it appears that $\partial T/\partial \mu = -v_{\infty 0}/(4B_0(1+\mu))$ at this end point. However, B_0 is unbounded as noted earlier. As will be clear from a discussion of the nature of the singularity in $\partial T/\partial \mu$ to be presented a little later, the correct form of the singularity is $\partial T/\partial \mu \sim (1+\mu)^{-3/4}$ at $\theta = \pi$. Consequently the integrand in [38] is zero at $\theta = \pi$. We have used this knowledge in calculating the values of the constants I_{n_0} reported in table 1.

Streamlines in a laboratory reference frame are displayed in figure 1. The topology of the flow field is virtually unchanged from that shown by Shankar & Subramanian (1988) for Ma = 200. The saddle point behind the bubble has moved closer to the bubble, when compared to their plot. Figure 1 clearly shows the transition from a potential dipole dominated flow field ahead of the bubble driven by the P_1 (Legendre) mode of the surface temperature distribution to that driven by the P_2 mode behind the bubble (see discussion in Shankar & Subramanian).

Table 1. The calculated values of the Fourier coefficients for the small Re flow field

n	I_n	n	I_n
2	−0.30761	14	−0.000747
3	0.06087	15	0.000624
4	−0.02557	16	−0.000528
5	0.01237	17	0.000451
6	−0.00750	18	−0.000389
7	0.00477	19	0.000339
8	−0.00334	20	−0.000297
9	0.00241	21	0.000262
10	−0.00182	22	−0.000233
11	0.00141	23	0.000208
12	−0.00112	24	−0.000187
13	0.000906	25	0.000169

The temperature drop over the bubble surface from the front pole to the rear pole may be shown to be

$$\Delta T = -\sum_{p=1}^{\infty} (4p-1) I_{2p} \qquad [47]$$

for the low Re flow field. This relation is obtained by integrating the tangential stress balance at the bubble surface $(\partial/\partial r)(v/r) = \partial T/\partial\theta$ at $r = 1$. From the form of the singularity mentioned above, it is seen that $(\partial T/\partial\theta)(1, \theta)$ at $\theta = \pi$ is integrable. Thus the series in [47] is expected to converge. Since the infinite series in [1] to [3] have been truncated at $n = N$ for numerical evaluation of I_n, the series in [47] is summed to the same level of truncation. Numerically determined values of ΔT for various N obtained in this manner are shown in figure 2. It is interesting that ΔT plotted versus $1/\sqrt{N}$ is fitted well by a straight line and extrapolates to a value very close to $\pi/2$ as $N \to \infty$.

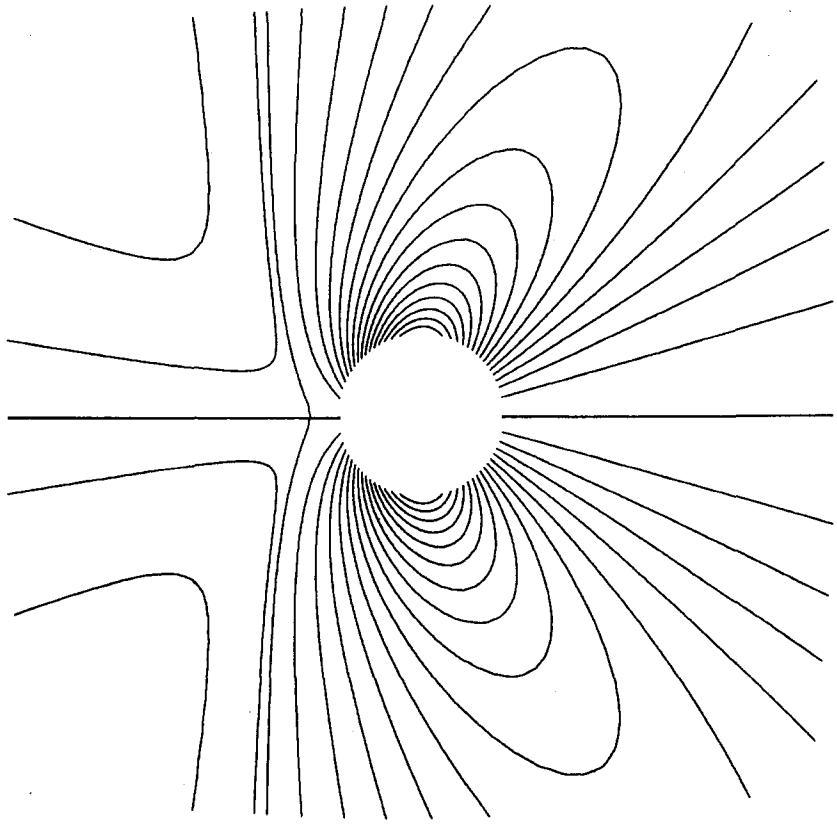

Figure 1. Streamlines (equally spaced in Ψ) in a laboratory reference frame for the case Re = 0, Ma → ∞. The values of the Fourier coefficients used to calculate the streamlines are given in table 1.

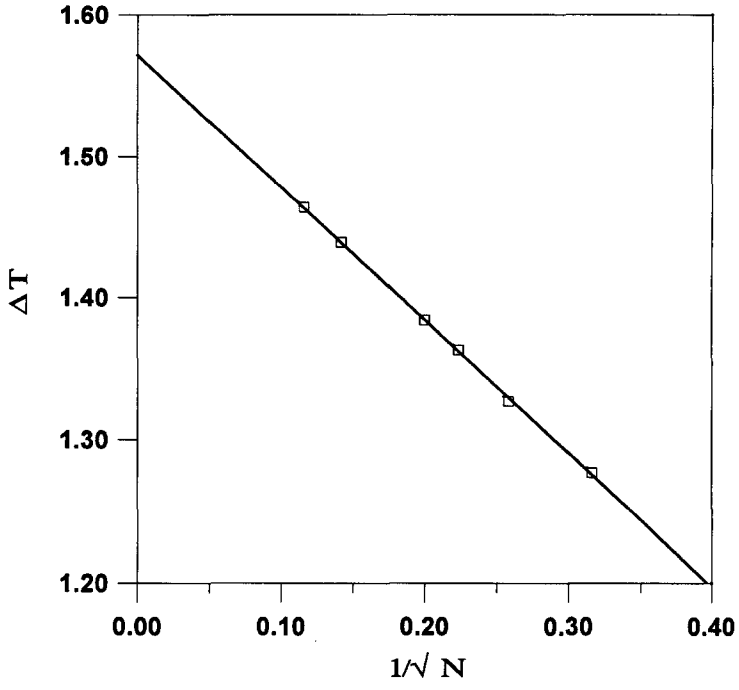

Figure 2. Scaled temperature difference, ΔT, over the bubble surface vs $1/\sqrt{N}$. N is the truncation level of the infinite series in [1]. The symbols (□) represent the actual values from numerical calculations. The straight line is a linear regression line. The intercept which represents ΔT for $N \to \infty$ is 1.5715 ± 0.00617 which is very close to $\pi/2$.

We discuss below the nature of the temperature singularity near the rear stagnation point. It must be stated at the outset that this singularity is unimportant in determining I_{n0}; the use of the Euler summation procedure has circumvented the convergence difficulties and enables the calculation of I_{n0}. This thermal singularity is produced because θ-conduction has been neglected in the energy equation near $\theta = \pi$. The scalings (i) $\mathbf{u} \cdot \nabla T \sim v_\infty \sim 1$ near the rear stagnation point and (ii) shear stress $\sim \nabla T$ (it turns out that for low Re the components of the stress tensor, in particular $\partial v/\partial\theta$, also scale as $|\nabla T|$) can be shown to yield $v \sim |\nabla T|^{-1} \sim (\pi - \theta)^{1/2} \sim (1 + \mu)^{1/4}$.

It is also possible to infer the nature of the singularity in $\partial T/\partial\mu$ from the calculated set I_{n_0}. In order to do this, we construct an analog of the Domb–Sykes plot used in the analysis of singularities of functions represented by power series (see Van Dyke 1975). Consider first the model function $1/(1 + \mu)^a$ for $0 < a < 1$. This can be expanded in a series of Legendre polynomials as follows

$$\frac{1}{(1+\mu)^a} = \sum_0^\infty H_n P_n(\mu) \qquad [48]$$

where

$$H_n = (-1)^n(2n + 1)2^{-a}\frac{\Gamma(1-a)}{\Gamma(a)}\frac{\Gamma(n+a)}{\Gamma(n+2-a)} \qquad [49]$$

A plot of H_n/H_{n-1} versus $1/n$ yields a straight line with the slope $(1 - 2a)$ for large n. The scaled viscous stress on the bubble surface can be written as

$$S(\mu) = -\frac{3}{2}\mu I_{2_0} - \frac{1}{2}\sum_{n=3}^{\infty} n(n-1)I_{n_0}P_{n-1}(\mu) \qquad [50]$$

By constructing a plot similar to that for the model function, one might guess that the singularity is the same as that of the model function. Such a plot is shown in figure 3 in the region where the ratios of the Fourier coefficients appear to be settling down after displaying oscillatory behavior for small values of n. The slope is 0.6 which gives a value $a = 1/5$, in contrast to the exact value $a = 1/4$. We believe that a greater precision is needed in I_{n_0} to extract the correct value of a from the numerical calculations.

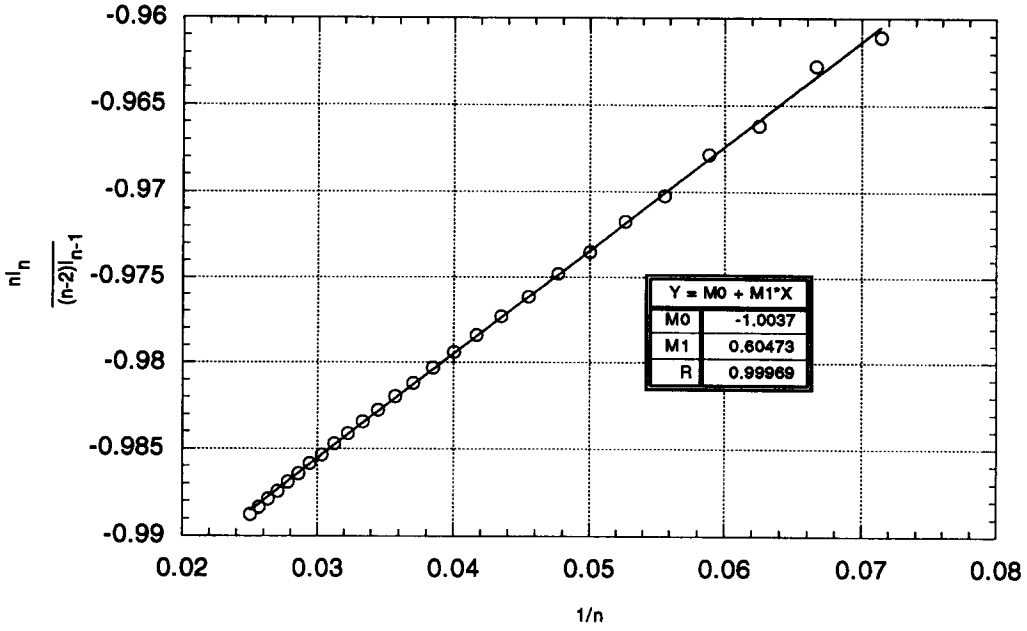

Figure 3. Plot of the ratios of successive Fourier coefficients vs $1/n$ for the infinite series in the expression for the normal stress in [50].

For the large Re flow field, the tangential stress balance cannot be satisfied without including the momentum boundary layer. Therefore a relation for ΔT analogous to [47] cannot be obtained. Also, the singularity in $\partial t/\partial\theta(1,\theta)$ at $\theta = \pi$ from [39] is not integrable. Hence the boundary layer in the angular direction near $\theta = \pi$ has to be analyzed carefully to determine ΔT over the bubble surface. This issue is addressed in appendix B.

4. HIGHER ORDER THERMAL BOUNDARY LAYER ANALYSIS

The leading order outer and inner temperature fields (T_0 and t_0) were analyzed in section 3. The higher order corrections in ϵ for the large Re flow field are calculated in this section. The chief assumption is that while Ma and Re are both large, the Prandtl number is small. That is, potential flow velocities are used in the convective terms in the energy equation and the viscous boundary layer contribution to energy dissipation is ignored. The consequence is that effects of order $O(\mathrm{Re}^{-1/2})$ are neglected. It is possible to obtain the proper $O(\epsilon)$ corrections to the temperature field since inclusion of the momentum boundary layer effects will yield corrections of $O(\epsilon \mathrm{Pr})$ which will be negligible for $\mathrm{Pr} \ll 1$. Hence the thermal corrections to the migration velocity are more important than corrections from the inclusion of the momentum boundary layer effects. As will be evident later, the analysis provides corrections to the bubble migration velocity at orders $O(\epsilon \ln \epsilon)$ and $O(\epsilon)$.

4.1. Outer temperature field

Let the outer temperature field be

$$T = T_0 + \epsilon T_1 + o(\epsilon). \qquad [51]$$

Here T_0 is the leading order outer temperature field given by [20]. Examining the governing equations for T, it can be verified that T_1 satisfies homogeneous equations and boundary conditions and is thus identically zero. Thus non-trivial corrections to T_0 occur only at $o(\epsilon)$. In section 3, T_0 was obtained via Taylor series expansions of the velocity fields in $(r-1)$. In this section we construct solutions to T_0 formally that are good to $O(\epsilon)$ when rewritten in inner variables. This is necessary in order to extend the inner solution to that order.

We note that T_0 may be expressed alternatively as

$$T_0(r,\theta) = G(\psi_0) - \int\left(\frac{2r^4}{2r^3+1}\right)\frac{d\theta}{\sin\theta} \qquad [52]$$

where the integrand in the indefinite integral must be expressed as a function of ψ_0 and θ. Since ψ_0 is a parameter in [20] and [52], one can expand T_0 about a given value of ψ_0, in particular $\psi_0 = 0$. We use [20] to expand T_0 in the vicinity of $\theta = 0$ and arbitrary r and [52] to expand T_0 in the vicinity of $r = 1$, $0 \leqslant \theta \leqslant \pi$. These two expressions for T_0 are then "patched" in the neighbourhood of $r = 1$ and $\theta = 0$ so that they are representations of the same function. This process yields $G(\psi_0) = a_0 + b_0 \ln\psi_0 + a_1\psi_0 + b_1\psi_0 \ln\psi_0$ and the values of the constants are determined by the patching procedure mentioned above. After a lengthy but straightforward calculation we may determine T_0 near $r = 1$ (up to $O(\psi_0)$) via [52] to be

$$\begin{aligned} T_0(r,\theta) = &\left(1 + \frac{\pi}{6\sqrt{3}} - \frac{1}{6}\ln 432\right) - \frac{1}{18}\left(\frac{\pi}{\sqrt{3}} + \ln 432\right)\left(r^2 - \frac{1}{r}\right)\sin^2\theta + \frac{1}{3}\ln\left(r^2 - \frac{1}{r}\right) \\ &+ \frac{2}{3}\ln(1+\cos\theta) + \frac{2}{9}\left(r^2 - \frac{1}{r}\right)\cos\theta + \frac{1}{9}\sin^2\theta\left(r^2 - \frac{1}{r}\right)\ln\left(r^2 - \frac{1}{r}\right) \\ &+ \frac{2}{9}\sin^2\theta\left(r^2 - \frac{1}{r}\right)\ln(1+\cos\theta) \end{aligned} \qquad [53]$$

We may now write T in inner variables as

$$\begin{aligned} T(x,\theta) = &\left(\frac{1}{3}\ln\epsilon\right) + \left(1 + \frac{\pi}{6\sqrt{3}} - \frac{1}{6}\ln 48 + \frac{1}{3}\ln x + \frac{2}{3}\ln(1+\cos\theta)\right) + \epsilon\ln\epsilon\left(\frac{1}{3}x\sin^2\theta\right) \\ &+ \epsilon\left(\frac{2}{3}x\cos\theta + \frac{1}{3}x\sin^2\theta\ln x + \frac{2}{3}x\sin^2\theta\ln(1+\cos\theta)\right. \\ &\left. - \frac{1}{6}\left(\frac{\pi}{\sqrt{3}} + \ln 48\right)x\sin^2\theta\right) \end{aligned} \qquad [54]$$

Thus the outer temperature field has correction terms at orders $\epsilon\ln\epsilon$ and ϵ when written in inner variables. This demonstrates that the next corrections to the inner field occur at $O(\epsilon\ln\epsilon)$ and $O(\epsilon)$. These are calculated below.

4.2. Inner temperature field

Let

$$v_\infty = v_{\infty 0} + \epsilon\ln\epsilon\, v_{\infty 11} + \epsilon v_{\infty 1} + o(\epsilon) \qquad [55]$$

$$t = \frac{1}{3}\ln\epsilon + t_0 + \epsilon\ln\epsilon\, t_{11} + \epsilon t_1 + o(\epsilon) \qquad [56]$$

t_0 has been obtained in section 3 ([39]). In what follows, we will obtain solutions for t_{11} and t_1 and also calculate $v_{\infty 11}$ and $v_{\infty 1}$. We use the match with [54] to establish boundary conditions on t_{11} and t_1 as $x \to \infty$.

4.2.1. Inner field at $O(\epsilon\ln\epsilon)$. From [8], the equation for t_{11} may be written as

$$v_{\infty 0}\left(-3x\cos\theta\frac{\partial t_{11}}{\partial x} + \frac{3}{2}\sin\theta\frac{\partial t_{11}}{\partial\theta}\right) = \frac{\partial^2 t_{11}}{\partial x^2} - \frac{v_{\infty 11}}{v_{\infty 0}}\frac{\partial^2 t_0}{\partial x^2} \qquad [57]$$

The boundary conditions are

$$\frac{\partial t_{11}}{\partial x} = 0 \quad \text{at } x = 0 \qquad [58]$$

$$t_{l1} \to \frac{1}{3} x \sin^2\theta \quad \text{as } x \to \infty \tag{59}$$

$$\frac{\partial t_{l1}}{\partial \theta} = 0 \quad \text{at } \theta = 0 \tag{60}$$

Equation [60] and a similar condition on t_1 follow from symmetry. The solution is

$$t_{l1} = -\frac{1}{6}\frac{v_{\infty l1}}{v_{\infty 0}} \mathrm{D}'(\zeta) + \frac{2}{9v_{\infty 0}}\left(\psi - 2\sqrt{\xi}\left(\zeta \operatorname{erfc}\zeta - \frac{1}{\sqrt{\pi}} \mathrm{e}^{-\zeta^2}\right)\right) \tag{61}$$

where $\psi = (\frac{3}{2})v_{\infty 0} x \sin^2\theta$, $\xi = (\frac{1}{2})v_{\infty 0}(1-\cos\theta)^2(2+\cos\theta)$ and $\zeta = \psi/(2\sqrt{\xi})$; ψ should really be ψ_0, but we omit the subscript in this section for convenience.

The contribution to the bubble velocity at $O(\epsilon \ln \epsilon)$ may be calculated from [7], [55] and [56] as

$$v_{\infty l1} = -\frac{1}{4}\int_0^{\pi}\left(\frac{\partial t_{l1}}{\partial \theta}\right)_{r=1} \sin^2\theta \, \mathrm{d}\theta$$

This yields

$$v_{\infty l1} = -\sqrt{\frac{1}{72\pi v_{\infty 0}}}\int_0^{\pi} \frac{\sin^5\theta}{(1-\cos\theta)(2+\cos\theta)^{1/2}} \mathrm{d}\theta$$

$$= -\sqrt{\frac{1}{72\pi v_{\infty 0}}}\left(\frac{16}{7}\sqrt{3} - \frac{64}{21}\right) = -0.1369 \tag{62}$$

4.2.2. Inner field at $O(\epsilon)$. The equation for t_1 can be obtained from [8] to be

$$v_{\infty 0}\left(2x - 3x\cos\theta\frac{\partial t_1}{\partial x} + \frac{3}{2}\sin\theta\frac{\partial t_1}{\partial \theta}\right) = \frac{\partial^2 t_1}{\partial x^2} + 2\frac{\partial}{\partial x}\left(x\frac{\partial t_0}{\partial x}\right) - \frac{v_{\infty 1}}{v_{\infty 0}}\frac{\partial^2 t_0}{\partial x^2} \tag{63}$$

with boundary conditions

$$\frac{\partial t_1}{\partial x} = 0 \quad \text{at } x = 0 \tag{64}$$

$$\frac{\partial t_1}{\partial \theta} = 0 \quad \text{at } \theta = 0 \tag{65}$$

and t_1 matches T_0 ([53]) far away. The solution can be found as the superposition of a particular solution and three homogeneous solutions $t_{1h1}, t_{1h2}, t_{1h3}$ that are constructed below.

- The particular solution is

$$t_{1p} = \frac{2}{3}x\left(\cos\theta + \sin^2\theta \ln\left(\frac{1+\cos\theta}{\sin\theta}\right)\right) - \frac{1}{6}\frac{v_{\infty 1}}{v_{\infty 0}}(1 - 2\zeta D(\zeta))$$

$$+ w(\theta)(-2\zeta + (4\zeta^2 - 2)\mathrm{D}(\zeta)) \tag{66}$$

where

$$w(\theta) = \frac{v_{\infty 0}}{2\xi^{3/2}}\left(\frac{2}{3}\cos\theta - \frac{1}{2}\cos^2\theta + \frac{1}{12}\cos^4\theta - \frac{1}{4}\right) \tag{67}$$

- At $\psi = 0$ $\partial t_{1h1}/\partial\psi = 0$; as $\psi \to \infty$ $t_{1h1} \to \left(\frac{2}{9v_{\infty 0}}\right)\left(\ln\left(\frac{4}{3v_{\infty 0}}\right) - \pi/(2\sqrt{3}) - \frac{1}{2}\ln 48\right)\psi$; at $\theta = 0$ $\partial t_{1h1}/\partial\theta = 0$. The solution is

$$t_{1h1} = \frac{2}{9v_{\infty 0}}\left(\ln\left(\frac{4}{3v_{\infty 0}}\right) - \frac{\pi}{2\sqrt{3}} - \frac{1}{2}\ln 48\right)\left(\psi - 2\sqrt{\xi}\left(\zeta \operatorname{erfc}\zeta - \frac{1}{\sqrt{\pi}}\mathrm{e}^{-\zeta^2}\right)\right) \tag{68}$$

- At $\psi = 0$ $t_{1h2} = 0$; as $\psi \to \infty$ $t_{1h2} \to (2/9(v_{\infty 0}))\psi \ln(\psi/2)$. The solution is

$$t_{1h2} = \frac{2}{9v_{\infty 0}}\left(\frac{\psi}{2}\ln\xi + \psi L(\zeta)\right) \quad [69]$$

where

$$(\zeta L')' + (1 + 2\zeta^2)L' = 2\zeta \quad [70]$$

$$L(\zeta) = \int_0^{\zeta} \frac{p - D(p)}{p^2}\,dp. \quad [71]$$

- At $\psi = 0$ $\partial t_{1h3}/\partial\psi = -(4/(9v_{\infty 0}))(\cos\theta/\sin^2\theta + \ln((1+\cos\theta)/\sin\theta)) + 2w(\theta)/\sqrt{\xi} - (\partial t_{1h2}/\partial\psi)_{\psi=0} \equiv K(\xi) + k/\sqrt{\xi}$; as $\psi \to \infty$ $t_{1h3} \to 0$; At $\theta = 0$ $\partial t_{1h3}/\partial\theta = 0$. k is chosen such that $K(\xi)$ is not singular at $\theta = 0$ and is given by

$$k = -\frac{20}{27}\left(\sqrt{\frac{3}{8v_{\infty 0}}}\right).$$

The fundamental solution that satisfies the condition $\partial P/\partial\psi = 1$ at $\psi = 0$, $P \to 0$ as $\psi \to \infty$ and $\partial P/\partial\theta = 0$ at $\theta = 0$ is

$$P(\psi, \xi) = 2\sqrt{\xi}\left(\zeta\,\mathrm{erfc}\,\zeta - \frac{1}{\sqrt{\pi}}\,e^{-\zeta^2}\right) \quad [72]$$

t_{1h3} can be obtained from Duhamel's theorem (Myers 1987) to be

$$\begin{aligned} t_{1h3}(\psi, \xi) &= -k\sqrt{\pi}\,\mathrm{erfc}\,\zeta + \int_0^{\xi} K(\tau)\frac{\partial P}{\partial\xi}(\psi, \xi - \tau)\,d\tau \\ &= -k\sqrt{\pi}\,\mathrm{erfc}\,\zeta - \frac{1}{\sqrt{\pi}}\int_0^{\xi}\frac{K(\tau)}{\sqrt{\xi - \tau}}\exp\left(-\frac{\psi^2}{4(\xi - \tau)}\right)d\tau \end{aligned} \quad [73]$$

The contribution to the bubble velocity at this order, $v_{\infty 1}$, is determined via [7], [55] and [56] to be $v_{\infty 1} = -\frac{1}{4}\int_0^{\pi}(\partial t_1/\partial\theta)(1, \theta)\sin^2\theta\,d\theta$. It can be shown that at $r = 1$, $(\partial t_1/\partial\theta) = (\partial t_{1h1}/\partial\theta) + (\partial t_{1h3}/\partial\theta)$. From [73], it can be determined that $t_{1h3}(1, \theta)$ has a logarithmic singularity near $\theta = \pi$. After integrating the expression for $v_{\infty 1}$ by parts we finally obtain $v_{\infty 1}$ to be

$$\begin{aligned} v_{\infty 1} = \frac{1}{3\sqrt{\pi}}\int_0^{\pi}\int_0^{\theta}\Bigg(&\ln\left(\frac{1+\cos\alpha}{\sin\alpha}\right) + \frac{\cos\alpha}{\sin^2\alpha} + \frac{3}{4}\frac{(3+\cos\alpha)}{(1-\cos\alpha)(2+\cos\alpha)^2} \\ &+ \frac{1}{4}\ln\tau + \frac{9kv_{\infty 0}}{4\sqrt{\tau}}\Bigg)\frac{\sin\theta\cos\theta\sin^3\alpha}{\sqrt{\xi(\theta) - \tau(\alpha)}}\,d\alpha\,d\theta \\ &- 0.1369\left(\ln\left(\frac{4}{3v_{\infty 0}}\right) - \frac{1}{2}\left(\frac{\pi}{\sqrt{3}} + \ln 48\right)\right) \end{aligned} \quad [74]$$

where $\tau(\alpha) = (v_{\infty 0}/2)(1 - \cos\alpha)^2(2 + \cos\alpha)$. The double integral is evaluated numerically. The result is

$$v_{\infty 1} = 0.5311 + 0.1267 = 0.6578 \quad [75]$$

Thus for the case $\mathrm{Re} \to \infty$, the result for the bubble migration velocity up to $O(\epsilon)$ is

$$v_{\infty} = \left(\frac{1}{3} - \frac{\ln 3}{8}\right) - 0.1369\epsilon\ln\epsilon + 0.6578\epsilon. \quad [76]$$

5. DISCUSSION

Crespo & Jiménez-Fernández (1992) report a leading order result $v_{\infty 0} = 0.223$ for the case of $\mathrm{Re} \to 0$. They mention using $N = 20$ for their calculations and report good convergence of the result.

While details of their numerical procedure to calculate the Fourier coefficients are not given, we suggest that the value reported by them is not correct. To establish this, we performed calculations for $N = 20$ with A_0 being calculated at every iteration without the benefit of the Euler summation and obtain $v_{\infty 0} = 0.2289$, $A_0 = 4.452$. $v_{\infty 0}$ is close to the value obtained by Crespo & Jiménez-Fernández (note: Crespo & Jiménez-Fernández do not report the value of A_0 and therefore this cannot be checked). In view of our comments in section 3.3.2, we do not believe this to be the converged value of $v_{\infty 0}$.

To establish the internal consistency of our results, we checked the equality of the left and right sides of the following equation obtained by integrating the energy equation ([8]), where [4] for I_n has been inserted

$$v_\infty(1 - 3v_\infty) = \frac{1}{4}\sum_{n=3}^{\infty} n(n-1)I_n^2 + \frac{1}{\mathrm{Ma}}\int_{-1}^{1} \frac{\partial^2 T}{\partial r^2}(1, \mu)\, \mathrm{d}\mu$$

$$= \frac{1}{4}\sum_{n=3}^{\infty} n(n-1)I_n^2 + \frac{1}{4A_0}\int_{-1}^{1} \frac{\xi'^2}{\xi}\, \mathrm{d}\mu \qquad [77]$$

This equation may also be obtained alternatively from the viscous dissipation arguments, mentioned in section 2, applied to the low Reynolds number velocity field. Our numerical results satisfy the above equation.

A key result from the present leading order analysis is that v_∞, the scaled bubble velocity, reaches an asymptotic limit for large Marangoni numbers. The limit for $\mathrm{Re} \to 0$ is smaller than that for $\mathrm{Re} \to \infty$ by 27.4%. This supports the behavior determined numerically by Balasubramaniam & Lavery (1989), who found the bubble velocity for $\mathrm{Ma} = 1000$ to increase with Re, though no asymptotic behavior was evident.

Shankar & Subramanian (1988) report that their scaled bubble velocity from numerical calculations under the creeping flow assumption decreases logarithmically with the Marangoni number. The extrapolated value from their curve fit to the numerical data is zero as the Marangoni number goes to infinity. We conclude that the behavior they predict is only true locally in the range of Ma in which the results were curve-fitted ($75 \leqslant \mathrm{Ma} \leqslant 200$).

The higher order analysis performed in section 4 shows that, at least for the large Re flow field, logarithmic dependence of the form $\epsilon \ln \epsilon$ occurs in the bubble velocity. Thus the approach to the asymptotic velocity is quite slow and the limit is attained only for very large Marangoni numbers. This explains why asymptotic behavior was not discerned in previous numerical simulations.

The solution for the thermal wake for large Re and Ma obtained in appendix B is interesting. The chief limitation of the analysis is that the use of potential flow velocities in the energy equation leads to a temperature drop over the bubble surface of order $O(\ln \epsilon)$ which is physically unrealistic. When the momentum wake analyzed in appendix A is taken into account in the thermal wake region, we speculate that this temperature drop will be of order $O(1)$.

6. CONCLUDING REMARKS

It has been demonstrated here that the scaled thermocapillary migration velocity approaches a non-zero asymptotic limit as the Marangoni number $\mathrm{Ma} \to \infty$. This is true in the two limits $\mathrm{Re} \to 0$ and $\mathrm{Re} \to \infty$. Given the nature of the results, it would be reasonable to conjecture that the statement holds true for any Re [see Crespo & Jiménez-Fernández (1992) who correctly comment that a similar analysis of the thermal boundary layer could analytically provide a boundary condition for the flow field for arbitrary Re]. We have also shown that the summations involved in the low Reynolds number problem must be handled carefully in order to arrive at the correct result for the migration velocity.

The analysis has also been extended to calculate the higher order corrections to the migration velocity for the case $\mathrm{Re} \to \infty$. Our principal result is that the next correction occurs at $O(\epsilon \ln \epsilon)$ and not at $O(\epsilon)$ as one might guess. While a similar extension is possible for $\mathrm{Re} \to 0$, the calculations for the Fourier coefficients appear formidable and we do not attempt them in this work.

The thermal wake has been analyzed for the case $\mathrm{Re} \to \infty$. In principle, the results can similarly be extended for $\mathrm{Re} \to 0$ as well. The thermal wake does not influence the bubble velocity up to $O(\epsilon)$.

REFERENCES

Abramowitz, M. & Stegun, I. 1968 *Handbook of Mathematical Functions*. Dover, New York.

Balasubramaniam, R. 1987 Thermocapillary bubble migration for large Marangoni numbers. NASA Contractor Report 179628, NASA Lewis Research Center, Cleveland, OH.

Balasubramaniam, R. & Chai, A. T. 1987 Thermocapillary migration of droplets: an exact solution for small Marangoni numbers. *J. Colloid Interface Sci.* **119,** 531–538.

Balasubramaniam, R. & Lavery, J. E. 1989 Numerical simulation of thermocapillary bubble migration under microgravity for large Reynolds and Marangoni numbers. *Numer. Heat Transfer A* **16,** 175–187.

Balasubramaniam, R. 1995 Thermocapillary bubble migration—solution of the energy equation for potential-flow approximated velocity fields. *Computational Fluid Dynamics* **3,** 407–414.

Bratukhin, Y. K. 1975 Thermocapillary drift of a viscous fluid droplet. *Iz. Akad. Nauk SSSR, Mech. Zh. Gaza* **5,** 156–161; original in Russian, NASA Technical Translation NASA TT 17093, 1976.

Burden, R. L., Faires, J. D. & Reynolds, A. C. 1981 *Numerical Analysis*. Wadsworth International Student Edition, Boston, MA.

Chao, B. T. 1962 Motion of spherical gas bubbles in a viscous fluid at large Reynolds numbers. *Phys. Fluids* **5,** 69–79.

Chen, J. C. & Lee, Y. T. 1992 Effect of surface deformation on thermocapillary bubble migration. *AIAA J.* **30,** 993–998.

Crespo, A. & Manuel, F. 1983 Bubble motion under reduced gravity. *Proc. 4th European Symposium on Materials Sciences Under Microgravity*, Madrid, Spain, pp. 45–49.

Crespo, A. & Jiménez-Fernández, J. 1992 Thermocapillary migration of bubbles at moderately large Reynolds numbers. In *Microgravity Fluid Mechanics* (Edited by Rath, H. J.), Proc. IUTAM Symposium Bremen 1991. Springer, Berlin.

Crespo, A. Jiménez-Fernández, J. 1992 Thermocapillary migration of bubbles: a semi-analytic solution for large Marangoni numbers. *Proc. 8th European Symposium on Materials and Fluid Sciences in Microgravity*, Brussels, Belgium.

Dill, L. H. & Balasubramaniam, R. 1992 Unsteady thermocapillary migration of isolated drops in creeping flow. *Int. J. Heat Fluid Flow* **13,** 78–85.

Haj-Hariri, H., Nadim, A. & Borhan, A. 1990 Effect of inertia on the thermocapillary velocity of a drop. *J. Colloid Interface Sci.* **140,** 277–286.

LeVan, M. D. & Newman, J. 1976 The effect of surfactant on the terminal and interfacial velocities of a bubble or drop. *AIChE J.* **22,** 695–701.

Levich, V. G. 1962 *Physicochemical Hydrodynamics*. Prentice–Hall, Englewood Cliffs, NJ.

Meksyn, D. 1961 *New Methods in Laminar Boundary-layer Theory*. Pergamon Press, New York.

Moore, D. W. 1963 The boundary layer on a spherical gas bubble. *J. Fluid Mech.* **16,** 161–176.

Myers, G. E. 1987 *Analytical Methods in Conduction Heat Transfer*. Genium, Schenectady, NY.

Nas, S. & Tryggvason, G. 1993 Computational investigation of thermal migration of bubbles and drops. AMD-Vol. 174/FED-Vol. 175, Fluid Mechanics Phenomena in Microgravity, ASME, New York.

Press, W. H., Flannery, B. P., Teukolsky, S. A. & Vetterling, W. T. 1986 *Numerical Recipes*. Cambridge University Press, London.

Shankar, N. & Subramanian, R. S. 1988 The Stokes motion of a gas bubble due to interfacial tension gradients at low to moderate Marangoni numbers. *J. Colloid Interface Sci.* **123,** 512–522.

Subramanian, R. S. 1981 Slow migration of a gas bubble in a thermal gradient. *AIChE J.* **27,** 646–654.

Subramanian, R. S. 1992 The motion of bubbles and drops in reduced gravity. In *Transport Processes in Bubbles, Drops and Particles* (Edited by Chhabra, R. P. & DeKee, D), pp. 1–42. Hemisphere, New York.

Szymczyk, J. & Siekmann, J. 1988 Numerical calculation of the thermocapillary motion of a bubble under microgravity. *Chem. Engng Commun.* **69,** 129–147.

Thompson, R. L., DeWitt, K. J. & Labus, T. L. 1980 Marangoni bubble motion phenomenon in zero gravity. *Chem. Engng Commun.* **5,** 299–314.
Van Dyke, M. 1975 *Perturbation Methods in Fluid Mechanics.* The Parabolic Press, Stanford, CA.
Wozniak, G., Siekmann, J. & Srulijes, J. 1988 Thermocapillary bubble and drop dynamics under reduced gravity—survey and prospects. *Z. Flugwiss. Weltraumforsch* **12,** 137–144.
Young, N. O., Goldstein, J. S. & Block, M. J. 1959 The motion of bubbles in a vertical temperature gradient. *J. Fluid Mech.* **6,** 350–356.

APPENDIX A

The Momentum Boundary Layer for Large Reynolds and Marangoni Numbers

The temperature field calculated in section 3 for the large Reynolds number flow field assumes that the velocities are given by the potential flow solution. We shall show below that this is a good assumption everywhere except near the rear stagnation point. There is a thin boundary layer near the bubble surface where the shear stress changes from that in potential flow (outside the boundary layer) to that demanded by the tangential balance at the bubble surface. This boundary condition is

$$r\frac{\partial}{\partial r}\left(\frac{v}{r}\right)=\frac{\partial T}{\partial \theta} \quad \text{at } r=1 \tag{A1}$$

From the result in section 3.3.1, the temperature gradient at the bubble surface is

$$\frac{\partial t_0}{\partial \theta}(1,\theta)\equiv T_s'(\theta)=-\frac{2}{3\sin\theta}+\frac{\sin^3\theta}{2(1-\cos\theta)^2(2+\cos\theta)} \tag{A2}$$

Following Moore (1963), the velocity field is written as the sum of the potential flow field and a boundary layer correction field. The momentum boundary layer problem is the same as in Moore's analysis, except for a change in the shear stress boundary condition.

$$U\frac{\partial v}{\partial r}+\frac{V}{r}\frac{\partial v}{\partial \theta}+\frac{1}{r}\frac{\partial V}{\partial \theta}v=\frac{1}{\mathrm{Re}}\frac{\partial^2 v}{\partial r^2} \tag{A3}$$

Here v is the θ-component of the velocity correction in the boundary layer; $\mathrm{Re}=(-\sigma_T)AR_1^2/(\mu\nu)$ is the Reynolds number; U, V are the potential flow velocity components near the bubble surface. Using suitable Taylor series expansions for U and V, the boundary value problem can be written as

$$v_{\infty 0}\left(-3(r-1)\cos\theta\frac{\partial v}{\partial r}+\frac{3}{2}\sin\theta\frac{\partial v}{\partial \theta}+\frac{3}{2}v\cos\theta\right)=\frac{1}{\mathrm{Re}}\frac{\partial^2 v}{\partial r^2} \tag{A4}$$

$$v=0 \quad \text{at } \theta=0 \text{ and as } r\to\infty \tag{A5}$$

$$\frac{\partial v}{\partial r}=3v_{\infty 0}\sin\theta+T_s'(\theta) \quad \text{at } r=1 \tag{A6}$$

The dependent and independent variables are transformed as follows:

$$p=\sqrt{\mathrm{Re}}\,v\sin\theta, \quad \chi=\frac{3}{2}\sqrt{\mathrm{Re}}\,v_{\infty 0}\sin^2\theta(r-1), \quad \xi=\frac{v_{\infty 0}}{2}(1-\cos\theta)^2(2+\cos\theta) \tag{A7}$$

This yields

$$\frac{\partial p}{\partial \xi}=\frac{\partial^2 p}{\partial \chi^2} \tag{A8}$$

$$p=0 \quad \text{at } \xi=0 \text{ and as } \chi\to\infty \tag{A9}$$

$$\frac{\partial p}{\partial \chi}=G(\xi)=2-\frac{4}{9v_{\infty 0}\sin^2\theta}+\frac{\sin^2\theta}{6\xi} \quad \text{at } \eta=0 \tag{A10}$$

It may be noticed that ξ is a time-like variable. The above "initial" value problem can be solved using Duhamel's theorem (Myers 1987). The fundamental solution, $P(\xi, \chi)$, which satisfies the boundary condition $\partial P/\partial\chi = 1$ at $\chi = 0$, is the same as Moore's solution and is

$$P(\xi, \chi) = \zeta \operatorname{erfc} \zeta - \frac{1}{\sqrt{\pi}} e^{-\zeta^2} \quad \zeta = \frac{\chi}{2\sqrt{\xi}} \tag{A11}$$

Thus by Duhamel's theorem

$$p(\xi, \chi) = \int_0^\xi G(\tau) \frac{\partial P}{\partial \xi}(\xi - \tau, \chi)\, d\tau = -\frac{1}{\sqrt{\pi}} \int_0^\xi \frac{G(\tau)}{\sqrt{\xi - \tau}} \exp\left(-\frac{\chi^2}{4(\xi - \tau)}\right) d\tau \tag{A12}$$

The expression for $G(\xi)$ ([A10]) is complicated and the Duhamel integral has to be evaluated numerically. Integrating $p(\xi, \chi)$ with respect to χ, the result for the volumetric flow rate in the boundary layer given by Crespo & Jiménez-Fernández (1991) can be recovered.

$p(\xi, \chi)$ given by [A12] is expected to be of order $O(1)$; consequently $v(r, \theta)$ in the momentum boundary layer scales as $\mathrm{Re}^{-1/2}$. Thus for large Re, the potential flow is only slightly perturbed in the momentum boundary layer [$O(1)$ changes occur only in the velocity gradient, i.e. stress]. It is therefore justified to include only the potential flow portion of the velocity field in the energy equation to calculate the temperature field. This is questionable near the rear stagnation point, where v from [A12] is expected to be singular.

APPENDIX B

The Thermal Wake for Large Reynolds and Marangoni Numbers

In section 3, it is seen that both the outer and inner temperature fields are singular at $\theta = \pi$. This happens for both the large and small Reynolds number flow fields. We shall attempt to remove this singularity by analyzing the tangential thermal boundary layer near $\theta = \pi$, for the case $\mathrm{Re} \to \infty$ using the potential flow velocities given in section 2.

The potential flow velocities given by [6] are not strictly valid in the thermal wake region. This is because the momentum boundary layer analyzed in appendix A will separate and form a flow wake in the vicinity of the rear stagnation point. Though the vorticity vanishes on the rear stagnation line $\theta = \pi$ and the flow field remains irrotational near it, the corrections to the velocities given by [6] will not be negligible in the wake. The flow wake will have a significant impact on the thermal wake. Balasubramaniam (1995) has compared the temperature profile in the thermal wake via numerical computations with and without the use of the potential flow velocities from [6] (numerically determined velocities are used in the latter case). He concluded that the two thermal wakes are drastically different away from the bubble. Nevertheless, for the purposes of this idealized analysis, we shall assume that the velocities are given by [6].

Outer temperature field

The temperature field in the absence of conduction must first be determined. This is done in a manner similar to the r-outer analysis performed in section 3.1 (we use the notation "r-outer" and "r-inner" to refer to the outer and inner solutions in the radial coordinate). The outer equation near $\theta = \pi$ is

$$1 + \left(1 - \frac{1}{r^3}\right)\frac{\partial T}{\partial r} - \frac{\phi}{r}\left(1 + \frac{1}{2r^3}\right)\frac{\partial T}{\partial \phi} = 0 \tag{B1}$$

where $\phi = \pi - \theta$ and $\phi \ll 1$. As $r \to \infty$, ∇T must attain the imposed uniform field and near the surface of the bubble, T must agree with the result in section 3.1 ([23]). The solution is

$$T_{\text{outer}} = C_3 + \frac{4}{3}\ln\phi - r + \frac{2}{3}\ln\left(r^2 - \frac{1}{r}\right) + \frac{1}{6}\ln\left(\frac{r^2 + r + 1}{(r-1)^2}\right) + \frac{1}{\sqrt{3}}\arctan\left(\frac{2r+1}{\sqrt{3}}\right) \tag{B2}$$

$$C_3 = 2 - \frac{\pi}{6\sqrt{3}} - \frac{1}{3}\ln 432 \tag{B3}$$

The outer field given above and the r-inner temperature field given by [39] are both singular at $\theta = \pi$. It is convenient to construct an r-composite field T_c near $\theta = \pi$ from these two results. The composite field serves as the ϕ-outer field for the thermal wake. However, it turns out that T_c constructed from [39] and [B2] is not valid in the vicinity of $\phi = 0$. Substitution of this T_c in [8] reveals that the remainder is proportional to $(r-1)(r^2-1)D'(\zeta)/r^4$, which is non-zero [i.e. $O(1)$] at $\phi = 0$ (i.e. $\zeta = 0$) and r not equal to 1 and therefore not tolerable. The source of this behavior is the $F(\hat{\zeta})$ term in [39]; its contribution to T_c is such that $\mathbf{u} \cdot \nabla T_c$ leaves the remainder given above. Fortunately, it is trivial to overcome this difficulty by seeking a solution in terms of the variable λ given below. $F(\lambda)$ has no contribution to the convective terms (λ is proportional to the stream function near $\theta = \pi$; $\hat{\zeta}$ is proportional to the stream function near $r = 1$). The composite temperature field may be written as

$$T_c = T_{\text{outer}} - \frac{2}{3}\ln\phi - \frac{1}{3}\ln\left(r^2 - \frac{1}{r}\right) + \frac{2}{3}F(\lambda) + \frac{1}{3}\ln\epsilon + \frac{1}{6}\ln\left(\frac{32}{v_{\infty 0}}\right) \tag{B4}$$

where

$$\lambda = \sqrt{\frac{\text{Ma}v_{\infty 0}}{32}}\left(r^2 - \frac{1}{r}\right)\phi^2 \tag{B5}$$

Inner temperature field

The equation for the temperature field in the wake including conduction in the tangential direction is (the inner variable is $y = \phi/\epsilon$)

$$v_{\infty 0}\left[1 + \left(1 - \frac{1}{r^3}\right)\frac{\partial t}{\partial r} - \frac{y}{r}\left(1 + \frac{1}{2r^3}\right)\frac{\partial t}{\partial y}\right] = \frac{1}{r^2 y}\frac{\partial}{\partial y}\left(y\frac{\partial t}{\partial y}\right) \tag{B6}$$

with boundary conditions

$$\frac{\partial t}{\partial y} = 0 \quad \text{at } y = 0 \tag{B7}$$

$$\frac{\partial t}{\partial r} = \text{finite} \quad \text{at } r = 1 \tag{B8}$$

and matching with T_c written above [note that $F(\lambda)$ rewritten in inner variables and truncated to $O(1)$ becomes $F(0)$ which is merely a constant]. An important observation with respect to the boundary condition in r is that at leading order t must not contain a term of the form $\ln(r-1)$ and thus $\partial t/\partial r$ must be finite at $r = 1$. We cannot impose $\partial t/\partial r = 0$ at $r = 1$ as this precludes the occurrence of higher order boundary layers (see section 4). An alternative boundary condition would be that the r-inner temperature field in the wake region [obtained by rewriting t in (x, y) coordinates and truncating to $O(1)$] must satisfy the adiabatic condition $\partial t/\partial x = 0$ at $x = 0$.

A similarity solution to t can be obtained to be

$$t(r, y) = C_3 + \frac{2}{3}F(0) + \frac{1}{6}\ln\frac{32}{v_{\infty 0}} + \ln\epsilon + \frac{2}{3}\ln y + \frac{1}{3}\ln\left(r^2 - \frac{1}{r}\right) + \frac{1}{6}\ln\left[\frac{r^2 + r + 1}{(r-1)^2}\right]$$
$$- r + \frac{1}{\sqrt{3}}\arctan\left(\frac{2r+1}{\sqrt{3}}\right) + \frac{1}{3}E_1\left[\frac{1}{4}v_{\infty 0}y^2\left(\frac{r^2 + r + 1}{r}\right)\right] \tag{B9}$$

where $E_1(x) = \int_x^\infty (e^{-p}/p)\,dp$ is an exponential integral (Abramowitz & Stegun 1968).

The composite solution in the wake is the same as t with $F(0)$ replaced by $F(\lambda)$. It is seen that while $\partial t/\partial r \to -1$ as $r \to \infty$, $t \to -r + \frac{2}{3}\ln r$. This behavior is tolerable at leading order, but points to difficulties that might arise at higher orders.

It can be shown that the temperature difference over the bubble surface from the forward to the rear stagnation points scales as $-\frac{2}{3}\ln\epsilon$, and is thus unbounded as $\text{Ma} \to \infty$. This agrees with the findings of Balasubramaniam (1995) who pointed out that this is a consequence of using the potential flow velocities in the energy equation. Indeed for the $\text{Re} \to 0$ flow field, ΔT over the bubble surface is finite ([47]), while for large Re, numerical calculations (Balasubramaniam & Lavery 1989) do not seem to indicate that ΔT is unbounded. It remains to be shown for large Re that when proper account is taken of the velocity corrections in the momentum wake, ΔT is indeed bounded.